Direct Electrochemistry of Molybdenum and Tungsten Enzymes

Vincent Fourmond

Direct electrochemistry of molybdenum and tungsten enzymes

Vincent Fourmond[a]

[a]*Aix-Marseille Université, CNRS, BIP UMR 7281, 31 chemin J. Aiguier, F-13402 Marseille cedex 20, France*

Abstract

Molybdenum and tungsten enzymes are almost omnipresent in living organisms; they catalyze a large variety of reactions on a large range of substrates, and are involved in a number of key cellular functions, like bacterial respiration, biological carbon, sulfur, and nitrogen cycles, detoxification. Most of these enzymes catalyze redox reactions, and they have successfully been connected to electrodes, in order to build biotechological devices like biosensors or biofuel cells, but also to learn about their catalytic properties, using protein film voltammetry, in which the electron transfer is direct and the enzymatic activity can be monitored as an electrical current. This chapter is an exhaustive review of the uses of direct electrochemistry for the study of molybdenum and tungsten enzymes.

Keywords: molybdenum enzymes; tungsten enzymes; direct electrochemistry; protein film voltammetry; nitrate reductase; sulfite oxidase

1. Introduction

For key reactions in their metabolism, living organisms use a number of transition metals, incorporated into metalloproteins. Among them, the only elements that do not belong to the first row are molybdenum and tungsten. These metals are used for the active site of nitrogenase, that catalyzes the reduction of N_2 to NH_3 at a complex $MoCFe_7S_9$ active site[1, 2], and are also incorporated in a series of recently discovered proteins of unkown function[3, 4]. Mostly, however, molybdenum and tungsten ions in metalloproteins are coordinated by one or two dithiolenes moeties from a pyranopterin-dithiolene ligand called "molybdopterin" (figure 1a). Enzymes incorporating such active sites are grouped in a large superfamily called mononuclear Mo (or W) enzymes[5, 6], because, with only one notable exception, the Mo or W ion is the only metal at the active site. This review focuses on enzymes of this superfamily; they will be referred to henceforth as "molybdoenzymes", regardless of the actual metal in the active site (Mo or W).

The molybdopterin cofactor in molybdoenzymes comes in several forms, either unmodified (in eukaryotes), or bound to a cytosine (pterin cytosine dinucleotide, PCD) or a guanosine (pterin guanosine dinucleotide, PGD), which are the forms of the cofactor used in prokaryotes. Phylogenetic data trace the ancestry of molybdoenzymes back to the last universal common ancestor[7], which suggest that they played an important role in the origin of life; however, which of molybdenum or tungsten was first used by organisms is still a matter of debate[8, 7].

Molybdoenzymes are able to process a large range of substrates. The reactions catalyzed are mostly (i) oxygen atom transfers[9], $RH + H_2O \rightleftharpoons ROH + 2\,H^+ + 2\,e^-$, like the reduction of nitrate, chlorate, selenate, and of N and S oxides

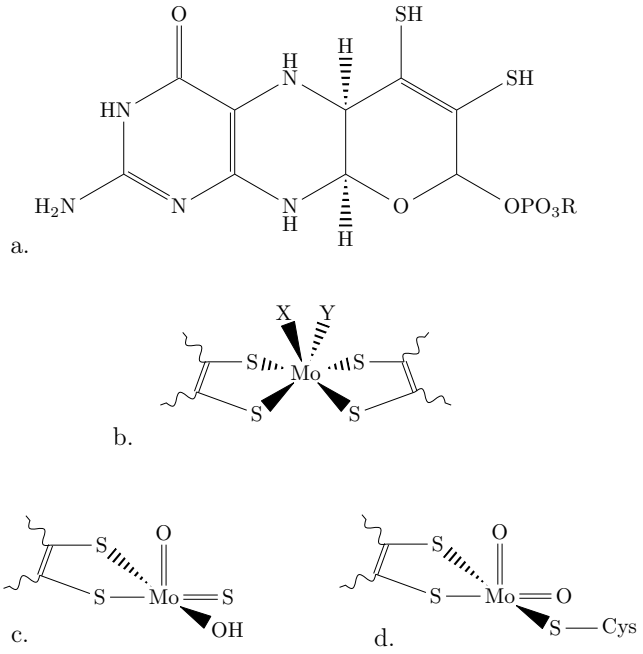

Figure 1: a. molybdopterin moiety (R can be H, guanosine dinucleotide, or cytosine dinucleotide). Active sites of b. Mo/W-*bis*PGD family (X is O or S, Y is Ser, Cys, SeCys or Asp), c. xanthine oxidase family, and d. sulfite oxidase family.

*To whom correspondance should be addressed. *Email address:* vincent.fourmond@imm.cnrs.fr, *Phone:* +33 4 91 16 45 36

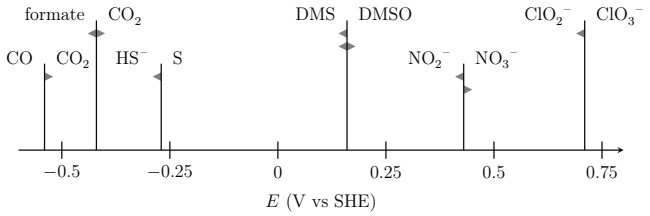

Figure 2: Small subset of the redox reactions catalyzed by molybdoenzymes, plotted on a potential scale (horizontal). The arrows indicate the direction of the reaction (oxidation or reduction); bidirectional arrows signify that a single enzyme catalyzes both the reduction and the oxidation. The potentials are taken from the list compiled in ref 11.

like DMSO, trimethylamine N-oxide (TMAO), biotin sulfoxide, and methionin sulfoxide, the oxidation of sulfite, arsenite, etc, and (ii) sulfur atom transfers, like the reduction of polysulfide or of thiosulfate. They also catalyze other reactions, like the reversible oxidation of formate to CO_2, some hydroxilations (like that of ethylbenzene), and even non-redox reactions, like the hydratation of acetylene[10]. A representative subset of the redox reactions catalyzed by molybdoenzymes are shown as a function of the reduction potential of the substrate in figure 2, which shows that molybdoenzymes are able to catalyze reactions spanning well over a volt.

The large range of reactions of molybdoenzymes is probably why they are used by almost all living organisms[12], for functions as diverse as the energetic metabolism, the assimilation of nitrogen (via the uptake of nitrate), the catabolism of purines and of sulfur-based amino acids, the detoxification of arsenite or selenate, the assimilation of carbon... As an example, molybdenum cofactor defiency in humans causes severe brain atrophy in newborn children, resulting in early death[13].

In the course of the catalytic reactions, the Mo and W ions are thought to cycle between the IV and VI redox states, potentially passing through an intermediate Mo(V) or W(V) state. These paramagnetic (V) states have been the subject of intense scrutiny with EPR spectroscopy to learn about the structure of the active site of many molybdoenzymes[11, 14, 15].

Molybdoenzymes are further divided into three subfamilies based on the structure of their oxidized active site (figure 1). In the Mo/W-*bis*PGD subfamily[11], exclusively found in prokaryotes, the Mo or W ion is coordinated by four sulfurs from two molybdopterins, a proteic ligand (in most of the members) and a sixth ligand, either an oxo or a sulfido group. The proteic ligand is either a serine, a cysteine (or selenocysteine), or an aspartate (figure 1b). The xanthine oxidase subfamily is characterized by a pentacoordinated Mo ion, with the two sulfides from a single dithiolene, equatorial sulfido and hydroxo and an apical oxo ligands (figure 1c). Finally, enzymes of the sulfite oxidase subfamily are characterized by a pentacoordinate geometry like in xanthine oxidase, with, in addition to the dithiolene ligand, an equatorial and an apical oxo ligand, and the thiolate of a cystein (figure 1d).

In addition to variations in the structure of their active site, molybdoenzymes host a great variety of other cofactors, like regular 4Fe4S, 3Fe4S, and 2Fe2S clusters, Rieske-type 2Fe2S

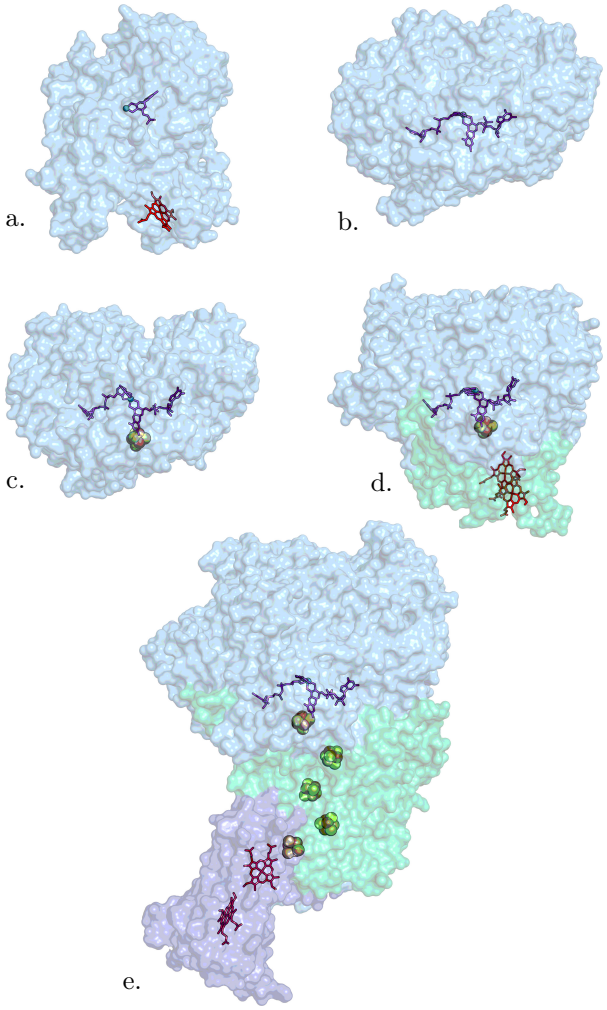

Figure 3: Structures of some of the molybdoenzymes discussed in text. a: chicken liver sulfite oxidase, PDB 1SOX[16]; b: *Rhodobacter capsulatus* DMSO reductase, PDB 3DMR[17]; c: *E. coli* formate dehydrogenase H, PDB 2IV2[18]; d: *Rhodobacter sphaeroides* periplasmic nitrate reductase, PDB 1GOY[19]; e: *E. coli* respiratory nitrate reductase A, PDB 1Q16[20]. All the structures are at the same scale, and the catalytic subunit from the Mo/W bis-PGD family are all displayed in the same orientation. The molybdenum cofactor is shown as purple sticks, hemes as red sticks, and iron-sulfur cofactors are shown as spheres.

clusters, hemes, etc. This diversity is exemplified by the structures shown in figure 3.

One of the most puzzling questions regarding molybdoenzymes is the relation between structure and function within the family, or rather the apparent lack thereof. For instance, periplasmic nitrate reductases and polysulfide reductases share the same active site: Mo-*bis*PGD with cystein as proteic ligand and sulfide as the sixth ligand, but they catalyze completely different reactions: the transfer of an oxygen atom for one, and that of a sulfur atom for the other. On the other hand, the reduction of nitrate is catalyzed by three very different molybdoenzymes: periplasmic nitrate reductases, respiratory nitrate reductases (which have an aspartate instead of the cystein as proteic ligand), and plant-type nitrate reductases, which are members

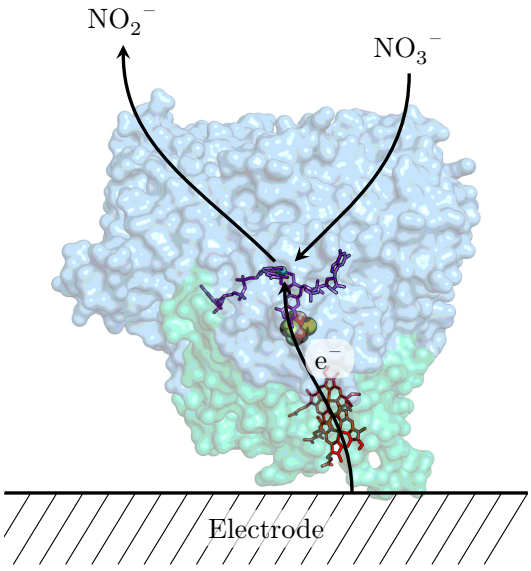

Figure 4: Schematic representation of Direct Electrochemistry, here using *Rhodobacter sphaeroides* NapAB as an example.

of the sulfite oxidase family, with only one molybdopterin in the coordination sphere of the molybdenum.

Besides, the specificity of substrate varies greatly among members of this family, with enzymes that process only a single substrate, while others can work with different substrates with almost the same rate; the respiratory nitrate reductase NarGH is for instance able to reduce both nitrate and chlorate with similar activities and values of K_m.

The broad range of substrates of the molybdoenzymes has attracted the interest of electrochemists who wish to tap into this large variety of reactions for analytic purposes[21], or for the construction of biofuel cells or devices for decontamination of water.

In this review, we focus on the electrochemistry of molybdoenzymes, and in particular on direct electrochemistry. In this technique, an enzyme is immobilized on an electrode in a configuration in which electron transfer is direct and fast between the electrode and the enzyme (figure 4), and the main purpose of the experiments is not to use the enzyme, but rather to learn about it[22–24]. We refer the reader to other reviews focussing on other aspects of the electrochemistry of molybdenum enzymes[25, 21].

This review is organized in two parts. The first is an exhaustive review of the direct electrochemistry of molybdoenzymes, system-by-system, while the second discusses specific topics addressed using protein film voltammetry across several systems.

2. Electrochemistry of molybdenum enzymes

2.1. Respiratory nitrate reductase

Respiratory nitrate reductases are members of the Mo/W bis-PGD subfamily; they are involved in anaerobic respiration using nitrate as the final electron acceptor, oxidizing quinols within the bacterial membrane; in *E. coli*, they are combined with respiratory formate dehydrogenases to form a redox loop and translocate protons across the cytoplasmic membrane[26]. *E. coli* respiratory nitrate reductase NarGHI is composed of three subunits (figure 3e): NarG (blue, top), which contains the molybdenum cofactor and a 4Fe4S cluster; NarH (green, middle), which contains four additional iron-sulfur clusters, and a NarI (purple, bottom), a membrane-anchored subunit that contains two hemes. NarG is the location of the reduction of nitrate, while the hemes in NarI oxidize quinols. The quinol oxidation site is versatile and able to work with several types of quinols of different reduction potentials[27]. The molybdenum ion in the active site is coordinated by the four sulfurs of the two molybdopterins, and an aspartate proteic ligand. The two subunits NarGH can be isolated independently of NarI to yield an enzyme that keeps its nitrate reduction activity, but has lost its ability to oxidize quinols. Most of the electrochemical studies of the respiratory nitrate reductase were performed on the NarGH subcomplex. In addition to nitrate, NarGH is able to reduce chlorate with slightly higher K_m and k_{cat} values, and also other substrates with lower activities.

The first molybdoenzyme ever studied using protein film voltammetry is *Paracoccus pantotrophus* (*Pp*) NarGH[28]. Anderson and coworkers characterized the dependence of the catalytic current (hence of the catalytic rate) on potential, nitrate concentration and pH, and quickly discovered that the enzymatic activity does not increase monotonously upon increasing the driving force (decreasing the potential), but that, in certain concentration ranges, *Pp* NarGH has a maximum of activity at intermediate potentials, and that decreasing the potential decreases the activity[29]. Elliott and coworkers demonstrated that these features are not specific to *Pp* NarGH, but that they are also visible in *E. coli* NarGH[30]. In fact, the wave shape is even more complex (figure 5a), with the presence of a peak at low concentrations of nitrate whose amplitudes saturates at lower concentrations than the low-potential plateau, giving complicated shapes in which the activity peaks, decreases and then increases again as the potential decreases (figure 5a, 125 µM). Maragon and coworkers also obtained complex waves with *Marinobacter hydrocarbonoclasticus* 617 NarGH, but did not observe peaks at intermediate potentials, only pronounced shoulders[31]. They recorded voltammograms in the presence of the alternative substrates chlorate and perchlorate, and showed that the wave shapes are very similar for all substrates, and that the positions of the features depend only slightly on the nature of the substrate and on its concentration[31].

Field and coworkers discovered that, under some conditions *Pp* NarGH activates the first time it is reduced[32], which could be observed by a very pronounced hysteresis in the first cyclic voltammogram, provided it was performed in the presence of nitrate. Ceccaldi and coworkers showed that this activation is also present in *E. coli* NarGH films, and that it proceeds in two steps: a reversible reaction involving neither electrons nor protons, followed by an irreversible reduction[33]. This activation had no effect on the spectroscopic signatures of the sample[33].

Respiratory nitrate reductases have been successfully immo-

bilized on graphite particles, and coupled to hydrogenases[34], to catalyze the oxidation of H_2 by nitrate, or combined with platinum or rhodium nanoparticles to catalyze the reduction of nitrate to ammonium[35].

2.2. Dissimilatory nitrate reductase

Another series of enzymes from the Mo/W bis-PGD family catalyze the reduction of nitrate to nitrite. They differ from the respiratory nitrate reductases in terms of overall architecture, active site coordination and physiological role. The archetypical dissimilatory nitrate reductase, *Rhodobacter sphaeroides* (*Rs*) NapAB, is composed of two subunits: NapA, that contains the molybdenum cofactor and a 4Fe4S cluster, and NapB, that contains two hemes[19] (figure 3d). In NapAB, the proteic ligand to the molybdenum is a cystein. The nature of the 6th ligand has long been a matter of debate, but it seems likely that the main EPR signatures of the enzymes correspond to structures in which the coordination sphere of the Mo ion is completed by a sulfide[43, 44]. However, whether these signatures are related to the active species is still an open question. Their physiological role is to dissipate excess in reducing power, to balance the redox potential of the quinone pool[45]. They are closely related to the bacterial assimilatory nitrate reductases, that have the same structural features, and whose role is to catalyze the first step in the assimilation of nitrate[45].

The first enzyme of this family to be immobilized on an electrode was the assimilatory nitrate reductase NarB from *Synechococcus* sp. PCC 7942. Butt and coworkers observed that much more reducing potentials are required to elicit catalysis from NarB than from NarGH, and proposed that this reflects differences in the source of electrons: quinones for NarGH vs ferredoxins for NarB[46, 47].

The dissimilatory nitrate reductase that has been studied the most using protein film voltammetry is *Rs* NapAB; it was observed early on that the nitrate reduction current generated by films of *Rs* NapAB shows a very pronounced optimum in an intermediate range of potential, and a plateau with lower activity at low potentials[36] (figure 5b). Frangioni and coworkers proposed a model in which the binding of nitrate to the active site is faster in the Mo(V) state than in the Mo(IV) state, and were able to quantitatively reproduce the experimental data[36]. This model was later extended by Bertrand and coworkers[48].

This marked optimum of potential is also present in *P. pantotrophus* NapAB[49], but is not visible when *Pp* NapAB reduces selenate rather than nitrate[50]. The shape of the voltammograms is visibly modified by the presence of azide[48, 49], or the introduction of point mutations in the environment of the active site[51], but the reasons for the change have not been elucidated yet. It has also been shown that the Michaelis constants depend strongly on potential[36, 52].

Both *Synechococcus* NarB[32] and *Rs* NapAB[53] activate the first time they are reduced. By a combination of PFV and EPR spectroscopy, it was shown that the species that activates gives the so called "high-*g* resting" EPR signature[53]; Jacques and coworkers showed that the chemical change occurs on the electronic path between the 4Fe4S cluster and the Mo, which point towards the involvement of the pterin in the activation process[54].

In addition to this first activation, *Rs* NapAB is reversibly inactivated under conditions of high potentials, low pH and high concentrations of nitrate[55]. Jacques and coworkers studied the kinetics of the formation of the inactive species, and concluded that the inactive species accumulate significantly, but probably not under paramagnetic redox states[56].

2.3. Formate dehydrogenases

Formate dehydrogenases catalyze the reversible oxidation of formate to carbon dioxide. They are closely related to dissimilatory nitrate reductases, with a selenocysteine in place of the cysteine ligand, and they most probably also have a sulfide as the 6th ligand to their active site. Thomé and coworkers showed that sulfuration of the soluble formate dehydrogenase FdhF from *E. coli*, either using exogenous sulfide or a dedicated sulfur transferase, was required for its activity[57]. Only two formate dehydrogenases were successfully connected to electrodes so far: the respiratory formate dehydrogenase from *Syntrophobacter fumaroxidans*, with a tungsten cofactor[58], and *E. coli* FdhF[37], which is part of the large hydrogen-formate lyase complex[59].

In both cases, the catalysis is fully reversible, with no overpotential in both directions. Reda and coworkers took advantage of this possibility to map the reduction potential of the CO_2/formate couple as a function of pH[58]. The wave shape of both Fdhs is simple, almost sigmoidal (figure 4e), and reminiscent of the ones observed with hydrogenases[60].

2.4. Sulfite oxidase and sulfite dehydrogenases

Sulfite oxidases, of course, compose the bulk of the "sulfite oxidase family"; they catalyze the oxidation of sulfite to sulfate. Eukaryotic sulfite oxidases are structured as a homodimer, and contain a heme in addition to the molybdenum cofactor. The first structure of chicken liver sulfite oxidase (figure 3a), lead to the puzzling remark that the heme cofactor is too far from the molybdenum (more than 30 Å) for direct electron transfer[16]. This lead to the proposal that the heme domain may exist in two conformations, an "open" conformation (the one crystallized), in which intramolecular electron transfer is not possible, but presumably the heme can interact with the redox partner, and a "closed" conformation in which the heme comes closer and intramolecular electron transfer is possible. Under this hypothesis, conformational changes would be necessary to evacuate the electrons from the active site. Support for this hypothesis came from flash photolysis experiments that showed that the intramolecular electron transfer rate is dependent on the solution viscosity, which suggests it is gated by a conformational change[61].

Elliott and coworkers were the first to wire sulfite oxidase (from chicken liver) to electrodes[38]. Sulfite oxidase gives "non-catalytic" (or "non-turnover") signals, which correspond to the exchange of electrons with the enzyme's redox cofactors, even in the absence of catalysis (inset of figure 5d). These signals inform on the reduction potential of the cofactors, and also

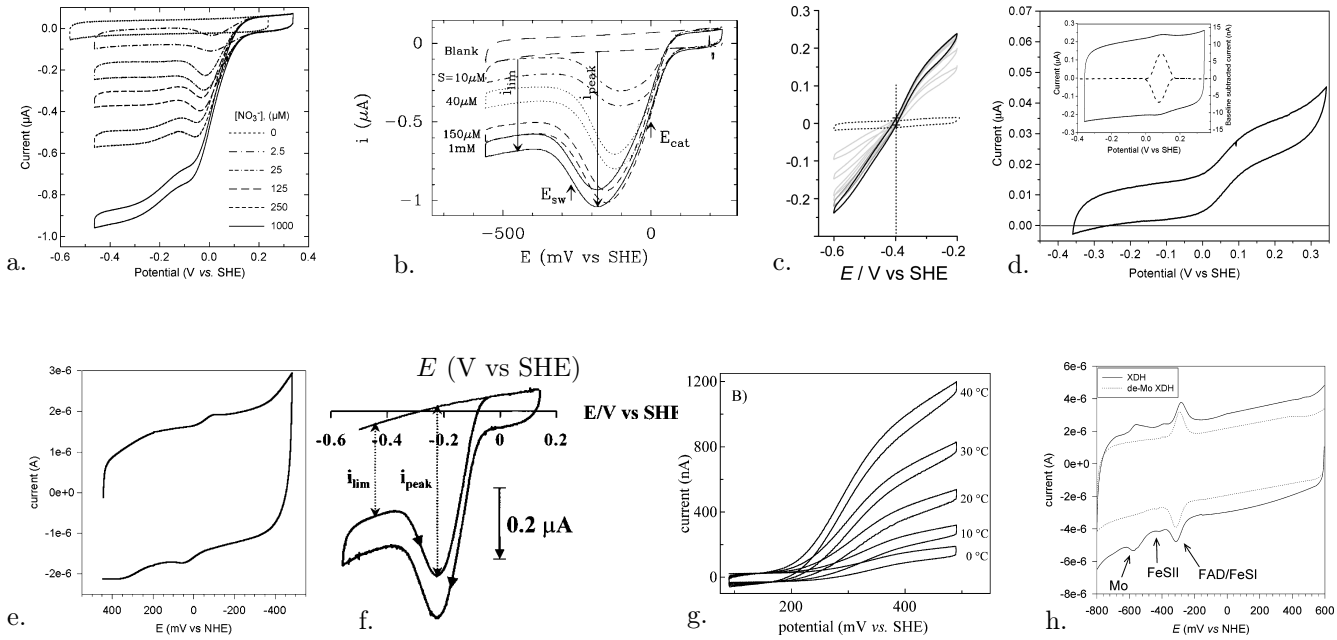

Figure 5: Representative voltammograms of molybdoenzymes. a. *E. coli* NarGH in the presence of nitrate, reprinted with permission from ref. 30, copyright 2004 American Chemical Society. b. *Rhodobacter sphaeroides* NapAB in the presence of nitrate, reprinted with permission from ref. 36, copyright 2004 American Chemical Society. c. *E. coli* FdhF, in the presence of both formate and CO_2, reprinted with permission from ref. 37, copyright 2014 American Chemical Society. d. chicken liver sulfite oxidase in the absence (inset) or presence of sulfite, reprinted with permission from ref. 38, copyright 2002 American Chemical Society. e. *Rhodobacter capsulatus* DMSO reductase, in the absence of any substrate, reprinted from ref. 39. f. *E. coli* DMSO reductase in the presence of DMSO, reprinted with permission from ref. 40, copyright 2001 American Chemical Society. g. *Alcaligenes faecalis* arsenite oxidase in the presence of arsenite, reprinted with permission from ref. 41, copyright 2004 American Chemical Society. h. *Starkeya novella* sulfite dehydrogenase in the absence of substrate, reprinted with permission from ref. 42, copyright 2003 American Chemical Society.

on the concentration of electroactive species at the electrode. This is important, since it makes it possible to determine absolute values of the turnover frequency on the electrode. In the case of sulfite oxidase, only the heme cofactor gives non-turnover signals, the Mo active site was never detected. In the presence of sulfite, a sigmoidal catalytic sulfite oxidation signal is observed (figure 4d), which corresponds to a turnover rate 20 times lower than that of the enzyme in solution, which lead Elliott and coworkers to the conclusion that most of the enzymes are locked in an inactive configuration in which the hemes are connected to the electrode, but never to the active site[38]. Ferapontova and coworkers used alkanethiol-modified gold electrodes, and studied the effect of the nature of the thiol on the catalytic current. They were able to obtain turnover rates nearly an order of magnitude higher than Elliott and coworkers, but still significantly lower that the values in solution[62].

Sezer and coworkers successfully immobilized human sulfite oxidase on thiol-modified silver electrode[63]. They obtained signals similar to those obtained for chicken sulfite oxidase, and were able to perform surface-enhanced Raman spectroscopy to detect the signals of the heme and titrate it[63]. They showed that the immobilization does not affect the heme's Raman signature, suggesting that the enzyme maintains its structural integrity on the electrode. Frasca and coworkers used a similar strategy to immobilize human sulfite oxidase on gold nanoparticles; they showed that this electrode has potential for applications in biosensors[64]. Zeng and coworkers were able to further improve this assembly by fine-tuning the coating of the nanoparticles, leading to improved rates of interfacial electron transfer between the heme and the electrode[65]. They also explored the possibility of making a sulfite/oxygen fuel cell using nanostructured gold electrodes[66], and wiring sulfite oxidase to quantum-dots modified indium tin oxide electrodes, in order to catalyze the photo-oxidation of sulfite[67]; a similar configuration was also recently used by Saengdee and coworkers to develop a sulfite biosensor[68].

Sulfite dehydrogenases are prokaryotic members of the sulfite oxidase family that catalyze the oxidation of sulfite to sulfate. They also contain a heme active site, but the overall fold is different from that of eukaryotic sulfite oxidases. Aguey-Zinsou and coworkers sucessfully adsorbed *Starkeya novella* sulfite dehydrogenase on PGE electrodes[42]; they obtained non-catalytic signals of both the heme and the molybdenum cofactors, whose potentials depended on the co-adsorbant used, and could demonstrate catalytic signals for the oxidation of sulfite[42]. Rapson and coworkers demonstrated that the catalytic wave shape of *Starkeya novella* sulfite dehydrogenase is not simply a sigmoid, but that it also presents a maximum in saturating concentrations of sulfite[69]. They studied the effect of active site point mutations on the shape of the voltammograms[70].

2.5. *Eukaryotic nitrate reductase*

Eukaryotic nitrate reductases are members of the sulfite oxidase family that reduce nitrate to nitrite as the first step in the

assimilation of nitrogen. They are found in plants and fungi, use NADH or NADPH as reducing equivalents, and harbor a heme and a FAD cofactor in addition to the molybdenum active site. Barbier and coworkers first reported sigmoidal catalytic voltammograms of reduction of nitrate from *Pichia angusta* nitrate reductase[71]. Kalimuthu and coworkers immobilized the nitrate reductase from the fungus *Neurospora crassa* on PGE electrodes, and could obtain non-catalytic signals of the heme and of dissociated FAD moeities, but not of the Mo center[72]. They observed catalytic reduction of nitrate, and determined the variation of the catalytic current as a function of nitrate concentration and of the pH. So far, no direct electrochemistry was reported on plant nitrate reductase; however, it should be noted that *Arabidopsis thaliana* nitrate reductase was studied by Kalimuthu and coworkers using redox mediators[73].

2.6. DMSO reductases

DMSO reductases, which reduce DMSO to DMS, are members of the Mo/W-*bis*PGD family, and are divided in two classes. DMSO reductases like that of *Rhodobacter capsulatus* (*Rc*) contain only the molybdenum center as single redox cofactor (figure 3b); their role is to dissipate excess reducing power. Aguey-Zinsou immobilized *Rc* DMSO reductase and successfully obtained non-catalytic signals (figure 5e); they could determine the reduction potential of both the Mo(VI)/(V) and the (V)/(IV) couples, and demonstrated that only the first reduction is coupled to a protonation[74]. They also obtained sigmoidal catalytic signals. They used the same approach to titrate the active site in two point mutants, Y114F, which has very little effect on the thermodynamics of the active site[75], and W116F (figure 5e), which does not affect the VI/V couple much, but results in the coupling of the V/IV reduction with a protonation[39].

Membrane-bound DMSO reductases like that of *E. coli* are much more complex, with no less than 5 iron-sulfur clusters and a quinone binding site in addition to the molybdenum cofactor. They are part of respiratory chains, similarly to NarGHI described above. Heffron and coworkers were the first to study them using protein film voltammetry; the catalytic wave of reduction of DMSO has a very marked optimum of potential (figure 5f), that correlates with the window of potential in which the Mo(V) EPR signal is observed, which lead to the proposition that the optimum of activity results from the Mo(V) being more reactive than Mo(IV)[40, 76, 77]. *E. coli* DMSO reductase does not oxidize DMS, but oxidizes trimethylphosphine, with an even more marked potential optimum.

2.7. Xanthine dehydrogenase/ xanthine oxidase

Xanthine oxidase/dehydrogenase oxidize xanthine to uric acid, and play a role in the degradation of purines; they oxidize a range of other substrates. They differ in whether oxygen (for xanthine oxidase) or NAD^+ (for xanthine dehydrogenase) is the electron acceptor. In some case, the dehydrogenase spontaneously converts to an oxidase.

Rhodobacter capsulatus xanthine dehydrogenase harbours 2 iron-sulfur clusters and a FAD, in addition to the molybdenum active site. Aguey-Zinsou and coworkers were the first to immobilize it on an electrode. They could detect non-catalytic signals in the range −600 to −200 mV, which they attributed to the Mo cofactor, one of the FeS cluster and the FAD[78]. They detected catalytic oxidation of xanthine, but at +400 mV, i.e. 600 mV higher than any non-catalytic signal, and far above the reduction potential of the acceptor, NAD^+ (around −300 mV). While the reason for such a discrepancy is still obscure, it is also observed in other systems, like the xanthine oxidase from bovine milk[79]. Kalimuthu and coworkers also demonstrated that electron transfer from xanthine dehydrogenase can be mediated by the product, uric acid[80].

Wu and coworkers immobilized bovine milk xanthine oxidase on single-wall carbon nanotube modified glassy carbon electrodes[81]. They could observe broad non-catalytic signals they attributed to all the cofactors, and detected catalytic currents of reduction of nitrate. Shan and coworkers immobilized xanthine oxidase using laponite nanoparticles, and were able to obtain well-defined signals attributed to the FAD cofactor, and an oxidation current in the presence of xanthine[82].

2.8. Other molybdoenzymes

Arsenite oxidases. They oxidize arsenite to arsenate. Hoke and coworkers studied *Alcaligenes faecalis* arsenite oxidase, and detected a single cooperative two-electron non-catalytic signal they attributed to the Mo center[41]. They could also record simple, almost sigmoidal, catalytic voltammograms of oxidation of arsenite (figure 5g).

Bernhardt and Santini immobilized the arsenite oxidase of the bacterium NT-26 on graphite electrodes, and were also able to monitor catalytic oxidation of arsenite, though they could not detect non-turnover signals[83]. This enzyme was also immobilized on multi-walled carbon nanotubes, for building an arsenite biosensor[84].

YedY. E. coli YedY is a member from the sulfite oxidase family. Gennaris and coworkers showed that it is involved in the defense against oxidative stress, by reducing protein-bound methionine sulfoxides[85]. Adamson and coworkers succesfully wired *E. coli* YedY to a PGE electrode, and could detect non-catalytic signals, one attributed to the Mo(V/IV) couple (Mo(VI) was never generated in solution) and one probably corresponding to a two-electron reduction of the pterin cofactor[86]; they could detect catalytic reduction of DMSO at a potential close to that of the pterin, which is the first indication that pterin ligand may play a redox role during catalysis in some molybdoenzymes[86, 87].

Aldehyde oxidoreductase. They belong to the xanthine oxidase family, and oxidize a variety of aldehydes; their physiological substrate and roles are often unknown. Correia dos Santos and coworkers were the first to report direct electrochemistry of an aldehyde oxidoreducase from *Desulfovibrio gigas*. They could detect the signatures of the iron-sulfur clusters when the enzyme is adsorbed on PGE electrodes, and that of the molybdenum center using a gold electrode and an enzyme in

solution[88]. A weak catalytic signal was observed in the presence of benzaldehyde, though, as it was a reduction current, its source is unclear.

Pinyou and coworkers succesfully embedded *E. coli* aldehyde oxidase PaoABC within redox hydrogels, and used it as anodes in vanillin/O_2 biofuel cells[89].

3. Overall topics in electrochemistry of molybdenum enzymes

3.1. Formation of films

Studying an enzyme with direct electrochemistry implies that one must be able to make electroactive films of the enzyme. Table 1 shows the strategies that were employed to obtain electroactive films in the articles described herein. Pyrolytic graphite edge electrodes are clearly the most used, often with a large variety of co-adsorbants, but gold electrodes have also been used successfully. It is hard to draw conclusions from this table: some systems seem to require a specific co-adsorbant (for instance, neomycin is required to obtain signals from dissimilatory nitrate reductases), while in some cases, the presence of a co-adsorbant is not necessary (for NarGH, for instance). Table 1 also shows that, while almost all the enzymes tested gave catalytic signals, only a small subset could give non-catalytic ones, and even less gave non-catalytic signals attributed to the Mo active site. The main purpose of table 1 is to provide inspiration for making films of not previously characterized enzymes.

3.2. Wave shapes

The dependence of the steady-state catalytic current generated by an enzyme film in the presence of its substrate is called the "wave shape". It closely resembles the steady-state enzymatic activity that enzymologists have learn to model and interpret since the discovery of enzymes, but with a much greater control on the driving force of the reaction via the electrode potential. The catalytic current is a complicated function of the rates of all the steps in the catalytic cycle, and it can therefore theoretically be interpreted to learn about all of them, or at least those whose rate can be varied: electron transfers, protonations, substrate binding, product release, provided the voltammograms are modelled quantitatively[90, 60].

Figure 5 shows that the wave shape of molybdenum enzymes is very varied, ranging from very simple sigmoidal shapes (figure 5d) to complex functions with local maxima and minima (figure 5a). The existence of a maximum in the curve, with the activity decreasing when the driving force increases past a certain threshold, is a puzzling feature of the catalytic wave shapes of molybdoenzymes, which is present in respiratory[29, 30] and dissimilatory nitrate reductases[36], respiratory DMSO reductase[40], but also under saturating conditions in sulfite dehydrogenase[69, 70], which shows that this feature is not limited to reductive catalysis[69]. This feature has been attributed to a faster binding of substrate (or protons) to the Mo(V) state than to the Mo(IV) state. Bertrand and coworkers have proposed the most complete model so far[48]. They derived the equations for the wave shape under the assumption of slow (and possibly reversible) substrate binding to all the redox states of

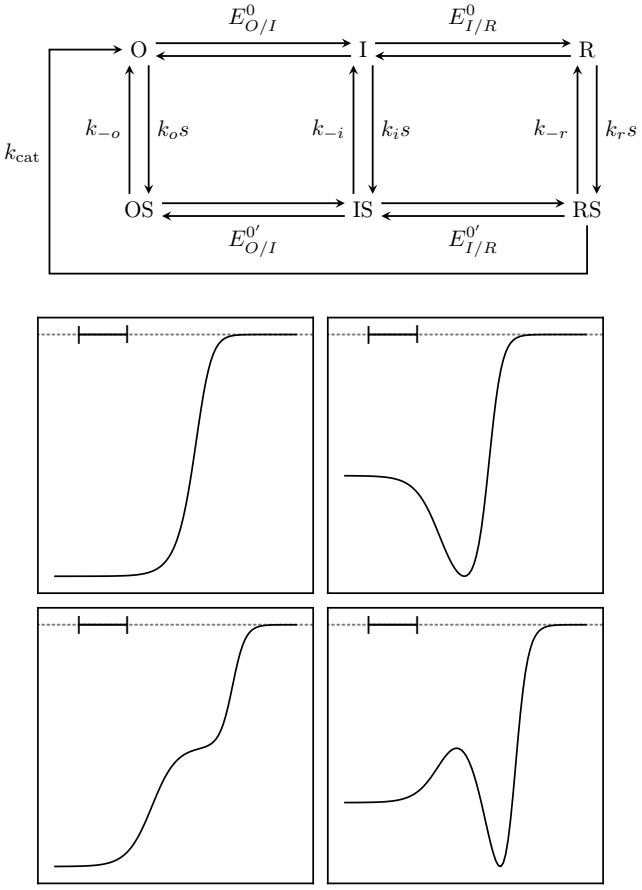

Figure 6: Top: model for the catalytic cycle proposed by Bertrand and coworkers[48], which features slow, reversible binding of substrate on all the redox of the active site. Bottom: examples of wave shapes obtained with different sets of parameters, the horizontal scale corresponds to 100 mV, and the horizontal dotted line corresponds to $i = 0$. Replotted with permission from ref. 48, copyright 2007 American Chemical Society.

the active site; they showed that this model has the complexity required to reproduce even the complex wave shapes of NarGH (figure 6), and they used it to quantitatively model the wave shapes of *Rs* NapAB[48]. However, the fits of this model for NapAB imply the existence of a stable Mo(V) species for the free active site, and it was later shown that it is not the case[53].

Wave shapes given by formate dehydrogenase (figure 5c) and arsenite oxidase (figure 5g) are much more simple, and resemble those obtained for hydrogenases[91, 60]; they have not been quantitatively modelled yet.

3.3. Activations/inactivations

Following the evolution of the activity over time as an enzyme activates or inactivates is very easy using direct electrochemistry, that samples the activity at high frequencies. The study of inactivation processes can sometimes provide lots of insights into the chemistry of the active site of enzymes[92, 93].

Another striking feature of molybdoenzymes is the observation that some of the enzymes activate or inactivate on the electrode in a potential dependent manner. These processes are sig-

Enzyme	species	electrode	co-adsorbant	non-cat	ref
NarGH	*P. pantotrophus*	PGE	neomycin		[28, 29, 32]
		gold	neomycin		[29]
	E. coli	PGE	polymixin		[30]
		PGE	(none)		[33]
		graphite particles	(none)		[34, 35]
	Marinobacter hydrocarbonoclasticus 617	PGE	neomycin		[31]
NarB	*Synechococcus* sp. PCC 7942	PGE	neomycin		[46, 47, 32]
		gold	mercaptopropionic acid & neomycin		[47]
NapAB	*R. sphaeroides*	PGE	neomycin		[36, 48, 53, 52, 54, 56, 55, 51]
	P. pantotrophus	PGE	neomycin		[49, 50]
NapA	*R. sphaeroides*	PGE	neomycin		[53]
Fdh	*Syntrophobacter fumaroxidans*	PGE	DDAB[a]		[58]
	E. coli	graphite-epoxy			[37]
Sulfite oxidase	chicken liver	PGE	(none)	heme	[38]
		gold	mercapto-6-hexanol	heme	[38]
		gold	alkanethiols	heme	[62]
	human	silver	thiols	heme	[63]
		gold nanoparticles	mercaptoundecanoic acid	heme	[64, 65]
		nanostructured gold	thiols	heme	[66]
		ITO + CdS quantum dots	(none)	heme	[67]
Sulfite dehydrogenase	*Starkeya novella*	PGE	DDAB or polylisine	heme & mo	[42]
		PGE	polylisine, PEI, kanamycin, or chitosan		[69, 70]
Nitrate reductase	*Pichia angusta*	PGE	polymixin		[71]
	Neurospora crassa	PGE	PEI + polymixin B	heme	[72]
DMSO reductase	*Rhodobacter capsulatus*	PGE	DDAB	Mo	[74, 75, 39]
	E. coli	PGE			[40, 76, 77]
Xanthine dehydrogenase	*R. capsulatus*	PGE		Mo, FeS, FAD	[78, 80]
Xanthine oxidase	bovine milk	PGE	DDAB	FAD	[79]
		SWCNT		broad signal	[81]
arsenite oxidase	*Alcaligens faecalis*	PGE		Mo	[41]
	NT-26	PGE	polymixin		[83]
		MWCNT-modified GC		Mo	[84]
YedY	*E. coli*	PGE		Mo, pterin	[86]
AOR	*D. gigas*	PGE		FeS	[88]

Table 1: Conditions used to make electroactive films of all enzymes described in this article, including the nature of the electrode and of the co-adsorbant (the latter includes thiols when applicable). The "non-cat" column describes whether non-turnover signals were observed, and to which redox center they were attributed. Abbreviations: PGE, pyrolytic graphite edge, DDAB, didodecyldimethylammonium bromide, PEI, polyethylene imine, ITO, indium tin oxide, SWCNT, single-wall carbon nanotubes, MWCNT, multi-wall carbon nanotubes, GC, glassy carbon. [a] whether DDAB is used or not is unclear in ref 58, since the methods refer to another article not describing the formation of films of *Sf* Fdh.

nificant, because they inform on the presence of inactive states that may be wrongly taken for active species in spectroscopic experiments. The most emblematic exemple is probably the Mo(V) "high *g* resting" state, that was thought to correspond to the Mo(V) state of the free active site, but was found instead to be an inactive form that activates the first time the enzyme is reduced[53], in which the pterin is probably oxidized[54]. Other enzymes like NarB[32] and NarGH[32, 33] also activate the first time they are reduced; this is reminiscent of the "redox cycling" process that activates DMSO reductases[94–96], also this activation has not been observed in electrochemical experiments yet. These first activation processes are easy to miss, since they disappear after the first reduction, it is possible that they may have been overlooked in other molybdoenzymes.

Finally, *Rs* also inactivates in the presence of large quantities of nitrate, in oxidizing conditions[55, 56], although the nature of the inactive species is still unclear. Nevertheless, the existence of such inactivations must be taken into account when designing experiments to trap catalytic intermediates to be characterized by spectroscopic techniques, to avoid mistaking inactive species for active ones.

4. Conclusion

This article provides an exhaustive review of the direct electrochemistry of molybdenum and tungsten enzymes. Molybdoenzymes have very rich electrochemical behaviours, with complex catalytic behaviours, the possibility to observe non-catalytic signals, and complex activation/inactivation processes. Their versatility in terms of subtrates processed and their high activities also make them good candidates for using in biotechnological devices like biosensors or biofuel cells.

Acknowledgments

The author acknowledges support from CNRS, Agence Nationale de la Recherche (ANR-12-BS08-0014, ANR-14-CE05-0010) and the A*MIDEX project (n° ANR-11-IDEX-0001-02) funded by the «Investissements d'Avenir» French Government program, managed by the French National Research Agency (ANR). The author is a member of the French Bioinorganic Chemistry group (http://frenchbic.cnrs.fr).

References

[1] T. Spatzal, M. Aksoyoglu, L. Zhang, S. L. A. Andrade, E. Schleicher, S. Weber, D. C. Rees, O. Einsle, Evidence for interstitial carbon in nitro-

genase FeMo cofactor., Science 334 (6058) (2011) 940. doi:10.1126/science.1214025.

[2] J. A. Wiig, Y. Hu, C. C. Lee, M. W. Ribbe, Radical SAM-dependent carbon insertion into the nitrogenase M-cluster., Science 337 (6102) (2012) 1672–1675. doi:10.1126/science.1224603.

[3] G. N. George, I. J. Pickering, E. Y. Yu, R. C. Prince, S. A. Bursakov, O. Y. Gavel, I. Moura, J. J. G. Moura, A novel protein-bound copper–molybdenum cluster, J. Am. Chem. Soc. 122 (34) (2000) 8321–8322. doi:10.1021/ja000955h.

[4] M. S. P. Carepo, S. R. Pauleta, A. G. Wedd, J. J. G. Moura, I. Moura, Mo-cu metal cluster formation and binding in an orange protein isolated from *Desulfovibrio gigas*., J. Biol. Inorg. Chem. 19 (4-5) (2014) 605–614. doi:10.1007/s00775-014-1107-8.

[5] S. Leimkühler, C. Iobbi-Nivol, Bacterial molybdoenzymes: old enzymes for new purposes., FEMS Microbiol. Rev. 40 (1) (2016) 1–18. doi:10.1093/femsre/fuv043.

[6] R. Hille, J. Hall, P. Basu, The mononuclear molybdenum enzymes, Chem. Rev. 114 (7) (2014) 3963–4038. doi:10.1021/cr400443z.

[7] B. Schoepp-Cothenet, R. van Lis, P. Philippot, A. Magalon, M. J. Russell, W. Nitschke, The ineluctable requirement for the trans-iron elements molybdenum and/or tungsten in the origin of life., Sci Rep 2 (2012) 263. doi:10.1038/srep00263.

[8] A. Kletzin, M. W. Adams, Tungsten in biological systems, FEMS Microbiology Reviews 18 (1996) 5–63. doi:10.1111/j.1574-6976.1996.tb00226.x.

[9] M. J. Pushie, J. J. Cotelesage, G. N. George, Molybdenum and tungsten oxygen transferases - structural and functional diversity within a common active site motif, Metallomics 6 (1) (2014) 15–24. doi:10.1039/c3mt00177f.

[10] G. B. Seiffert, G. M. Ullmann, A. Messerschmidt, B. Schink, P. M. H. Kroneck, O. Einsle, Structure of the non-redox-active tungsten/[4Fe:4S] enzyme acetylene hydratase, Proc. Natl Acad. Sci. USA 104 (9) (2007) 3073–3077. doi:10.1073/pnas.0610407104.

[11] S. Grimaldi, B. Schoepp-Cothenet, P. Ceccaldi, B. Guigliarelli, A. Magalon, The prokaryotic Mo/W-*bis*PGD enzymes family: a catalytic workhorse in bioenergetic, Biochim. Biophys. Acta 1827 (8-9) (2013) 1048–1085. doi:10.1016/j.bbabio.2013.01.011.

[12] Y. Zhang, V. N. Gladyshev, Molybdoproteomes and evolution of molybdenum utilization, J. Mol. Biol. 379 (4) (2008) 881–899. doi:10.1016/j.jmb.2008.03.051.

[13] B. C. Schwahn, F. J. Van Spronsen, A. A. Belaidi, S. Bowhay, J. Christodoulou, T. G. Derks, J. B. Hennermann, E. Jameson, K. König, T. L. McGregor, E. Font-Montgomery, J. A. Santamaria-Araujo, S. Santra, M. Vaidya, A. Vierzig, E. Wassmer, I. Weis, F. Y. Wong, A. Veldman, G. Schwarz, Efficacy and safety of cyclic pyranopterin monophosphate substitution in severe molybdenum cofactor deficiency type a: a prospective cohort study, The Lancet 386 (2015) 1955–1963. doi:10.1016/S0140-6736(15)00124-5.

[14] R. A. Rothery, G. J. Workun, J. H. Weiner, The prokaryotic complex iron-sulfur molybdoenzyme family, Biochim. Biophys. Acta 1778 (2008) 1897–1929. doi:10.1016/j.bbamem.2007.09.002.

[15] M. J. Pushie, G. N. George, Spectroscopic studies of molybdenum and tungsten enzymes, Coord. Chem. Rev. 255 (9-10) (2011) 1055–1084. doi:10.1016/j.ccr.2011.01.056.

[16] C. Kisker, H. Schindelin, A. Pacheco, W. A. Wehbi, R. M. Garrett, K. V. Rajagopalan, J. H. Enemark, D. C. Rees, Molecular basis of sulfite oxidase deficiency from the structure of sulfite oxidase, Cell 91 (7) (1997) 973–983. doi:10.1016/S0092-8674(00)80488-2.

[17] A. S. McAlpine, A. G. McEwan, A. L. Shaw, S. Bailey, Molybdenum active centre of dmso reductase from rhodobacter capsulatus : crystal structure of the oxidised enzyme at 1.82-Å resolution and the dithionite-reduced enzyme at 2.8-Å resolution, Journal of Biological Inorganic Chemistry 2 (1997) 690–701. doi:10.1007/s007750050185.

[18] H. Raaijmakers, M. Romão, Formate-reduced *E. coli* formate dehydrogenase H: the reinterpretation of the crystal structure suggests a new reaction mechanism, J. Biol. Inorg. Chem. 11 (7) (2006) 849–854. doi:10.1007/s00775-006-0129-2.

[19] P. Arnoux, M. Sabaty, J. Alric, B. Frangioni, B. Guigliarelli, J.-M. Adriano, D. Pignol, Structural and redox plasticity in the heterodimeric periplasmic nitrate reductase, Nat. Struct. Mol. Biol. 10 (11) (2003) 928–934. doi:10.1038/nsb994.

[20] M. G. Bertero, R. A. Rothery, M. Palak, C. Hou, D. Lim, F. Blasco, J. H. Weiner, N. C. J. Strynadka, Insights into the respiratory electron transfer pathway from the structure of nitrate reductase A, Nat. Struct. Mol. Biol. 10 (9) (2003) 681–687. doi:10.1038/nsb969.

[21] P. V. Bernhardt, Exploiting the versatility and selectivity of mo enzymes with electrochemistry, Chem. Commun. 47 (6) (2011) 1663–1673. doi:10.1039/c0cc03681a.

[22] C. Léger, P. Bertrand, Direct electrochemistry of redox enzymes as a tool for mechanistic studies, Chem. Rev. 108 (7) (2008) 2379–2438. doi:10.1021/cr0680742.

[23] F. A. Armstrong, H. A. Heering, J. Hirst, Reactions of complex metalloproteins studied by protein-film voltammetry, Chem. Soc. Rev. 26 (1997) 169–179. doi:10.1039/CS9972600169.

[24] V. Fourmond, C. Léger, Protein electrochemistry: Questions and answers., Adv. Biochem. Eng. Biotechnol. 158 (2016) 1–41. doi:10.1007/10_2015_5016.

[25] R. D. Milton, S. D. Minteer, Enzymatic bioelectrosynthetic ammonia production: Recent electrochemistry of nitrogenase, nitrate reductase and nitrite reductase, ChemPlusChemdoi:10.1002/cplu.201600442.

[26] M. Jormakka, S. Tornroth, B. Byrne, S. Iwata, Molecular basis of proton motive force generation: Structure of formate dehydrogenase-N, Science 295 (5561) (2002) 1863–1868. doi:10.1126/science.1068186.

[27] J. Rendon, E. Pilet, Z. Fahs, F. Seduk, L. Sylvi, M. Hajj Chehade, F. Pierrel, B. Guigliarelli, A. Magalon, S. Grimaldi, Demethylmenaquinol is a substrate of *Escherichia coli* nitrate reductase A (NarGHI) and forms a stable semiquinone intermediate at the NarGHI quinol oxidation site., Biochim. Biophys. Acta 1847 (8) (2015) 739–747. doi:10.1016/j.bbabio.2015.05.001.

[28] L. J. Anderson, D. J. Richardson, J. N. Butt, Using direct electrochemistry to probe rate limiting events during nitrate reductase turnover., Faraday Discuss. 116 (116) (2000) 155–69. doi:10.1039/b000946f.

[29] L. Anderson, D. Richardson, J. Butt, Catalytic protein film voltammetry from a respiratory nitrate reductase provides evidence for complex electrochemical modulation of enzyme activity., Biochemistry 40 (38) (2001) 11294–307. doi:10.1021/bi002706b.

[30] S. Elliott, K. Hoke, K. Heffron, M. Palak, R. Rothery, J. Weiner, F. Armstrong, Voltammetric studies of the catalytic mechanism of the respiratory nitrate reductase from *Escherichia coli*: How nitrate reduction and inhibition depend on the oxidation state of the active site, Biochemistry 43 (3) (2004) 799–807. doi:10.1021/bi035869j.

[31] J. Marangon, P. M. Paes de Sousa, I. Moura, C. D. Brondino, J. J. G. Moura, P. J. González, Substrate-dependent modulation of the enzymatic catalytic activity: Reduction of nitrate, chlorate and perchlorate by respiratory nitrate reductase from *Marinobacter hydrocarbonoclasticus* 617, Biochim. Biophys. Acta 1817 (7) (2012) 1072–1082. doi:10.1016/j.bbabio.2012.04.011.

[32] S. J. Field, N. P. Thornton, L. J. Anderson, A. J. Gates, A. Reilly, B. J. N. Jepson, D. J. Richardson, S. J. George, M. R. Cheesman, J. N. Butt, Reductive activation of nitrate reductases., Dalton Trans. (21) (2005) 3580–3586. doi:10.1039/b505530j.

[33] P. Ceccaldi, J. Rendon, C. Léger, R. Toci, B. Guigliarelli, A. Magalon, S. Grimaldi, V. Fourmond, Reductive activation of *E. coli* respiratory nitrate reductase, Biochim. Biophys. Acta 1847 (10) (2015) 1055–1063. doi:10.1016/j.bbabio.2015.06.007.

[34] K. A. Vincent, X. Li, C. F. Blanford, N. A. Belsey, J. H. Weiner, F. A. Armstrong, Enzymatic catalysis on conducting graphite particles., Nat. Chem. Biol. 3 (12) (2007) 761–762. doi:10.1038/nchembio.2007.47.

[35] M. Duca, J. R. Weeks, J. G. Fedor, J. H. Weiner, K. A. Vincent, Combining noble metals and enzymes for relay cascade electrocatalysis of nitrate reduction to ammonia at neutral ph, ChemElectroChem 2 (2015) 1086–1089. doi:10.1002/celc.201500166.

[36] B. Frangioni, P. Arnoux, M. Sabaty, D. Pignol, P. Bertrand, B. Guigliarelli, C. Léger, In *Rhodobacter sphaeroides* respiratory nitrate reductase, the kinetics of substrate binding favors intramolecular electron transfer, J. Am. Chem. Soc. 126 (5) (2004) 1328–9. doi:10.1021/ja0384072.

[37] A. Bassegoda, C. Madden, D. W. Wakerley, E. Reisner, J. Hirst, Reversible interconversion of CO_2 and formate by a molybdenum-containing formate dehydrogenase, J. Am. Chem. Soc. 136 (44) (2014) 15473–15476. doi:10.1021/ja508647u.

[38] S. J. Elliott, A. E. McElhaney, C. Feng, J. H. Enemark, F. A. Arm-

strong, A voltammetric study of interdomain electron transfer within sulfite oxidase., J. Am. Chem. Soc. 124 (39) (2002) 11612–3. doi:10.1021/ja027776f.

[39] J. P. Ridge, K.-F. Aguey-Zinsou, P. V. Bernhardt, G. R. Hanson, A. G. McEwan, The critical role of tryptophan-116 in the catalytic cycle of dimethylsulfoxide reductase from *Rhodobacter capsulatus*, FEBS Lett. 563 (1-3) (2004) 197–202. doi:10.1016/S0014-5793(04)00301-1.

[40] K. Heffron, C. Léger, R. Rothery, J. Weiner, F. Armstrong, Determination of an optimal potential window for catalysis by *E. coli* dimethyl sulfoxide reductase and hypothesis on the role of Mo(V) in the reaction pathway, Biochemistry 40 (10) (2001) 3117–3126. doi:10.1021/bi002452u.

[41] K. Hoke, N. Cobb, F. Armstrong, R. Hille, Electrochemical studies of arsenite oxidase: An unusual example of a highly cooperative two-electron molybdenum center, Biochemistry 43 (6) (2004) 1667–1674. doi:10.1021/bi0357154.

[42] K.-F. Aguey-Zinsou, P. V. Bernhardt, U. Kappler, A. G. McEwan, Direct electrochemistry of a bacterial sulfite dehydrogenase., J. Am. Chem. Soc. 125 (2) (2003) 530–5. doi:10.1021/ja028293e.

[43] S. Najmudin, P. González, J. Trincão, C. Coelho, A. Mukhopadhyay, N. Cerqueira, C. Romão, I. Moura, J. Moura, C. Brondino, M. Romão, Periplasmic nitrate reductase revisited: a sulfur atom completes the sixth coordination of the catalytic molybdenum, J. Biol. Inorg. Chem. 13 (5) (2008) 737–753. doi:10.1007/s00775-008-0359-6.

[44] F. Biaso, B. Burlat, B. Guigliarelli, DFT investigation of the molybdenum cofactor in periplasmic nitrate reductases: Structure of the Mo(V) EPR-active species, Inorg. Chem. 51 (6) (2012) 3409–3419. doi:10.1021/ic201533p.

[45] B. J. N. Jepson, A. Marietou, S. Mohan, J. A. Cole, C. S. Butler, D. J. Richardson, Evolution of the soluble nitrate reductase: defining the monomeric periplasmic nitrate reductase subgroup., Biochem. Soc. Trans. 34 (Pt 1) (2006) 122–126. doi:10.1042/BST0340122.

[46] J. N. Butt, L. J. Anderson, L. M. Rubio, D. J. Richardson, E. Flores, A. Herrero, Enzyme-catalysed nitrate reduction–themes and variations as revealed by protein film voltammetry, Bioelectrochemistry 56 (1-2) (2002) 17–18. doi:10.1016/S1567-5394(02)00049-X.

[47] B. J. N. Jepson, L. J. Anderson, L. M. Rubio, C. J. Taylor, C. S. Butler, E. Flores, A. Herrero, J. N. Butt, D. J. Richardson, Tuning a nitrate reductase for function: The first spectropotentiometric characterization of a bacterial assimilatory nitrate reductase reveals novel redox properties, J. Biol. Chem. 279 (31) (2004) 32212–32218. doi:10.1074/jbc.M402669200.

[48] P. Bertrand, B. Frangioni, S. Dementin, M. Sabaty, P. Arnoux, B. Guigliarelli, D. Pignol, C. Léger, Effects of slow substrate binding and release in redox enzymes: Theory and application to periplasmic nitrate reductase, J. Phys. Chem. B 111 (34) (2007) 10300–10311. doi:10.1021/jp074340j.

[49] A. J. Gates, D. J. Richardson, J. N. Butt, Voltammetric characterization of the aerobic energy-dissipating nitrate reductase of *Paracoccus pantotrophus*: exploring the activity of a redox-balancing enzyme as a function of electrochemical potential, Biochem. J. 409 (1) (2008) 159–168. doi:10.1042/BJ20071088.

[50] A. J. Gates, C. S. Butler, D. J. Richardson, J. N. Butt, Electrocatalytic reduction of nitrate and selenate by napab., Biochem. Soc. Trans. 39 (1) (2011) 236–242. doi:10.1042/BST0390236.

[51] V. Fourmond, B. Burlat, S. Dementin, M. Sabaty, P. Arnoux, E. Étienne, B. Guigliarelli, P. Bertrand, D. Pignol, C. Léger, Dependence of catalytic activity on driving force in solution assays and protein film voltammetry: Insights from the comparison of nitrate reductase mutants, Biochemistry 49 (11) (2010) 2424–2432. doi:10.1021/bi902140e.

[52] V. Fourmond, T. Lautier, C. Baffert, F. Leroux, P.-P. Liebgott, S. Dementin, M. Rousset, P. Arnoux, D. Pignol, I. Meynial-Salles, P. Soucaille, P. Bertrand, C. Léger, Correcting for electrocatalyst desorption or inactivation in chronoamperometry experiments, Anal. Chem. 81 (8) (2009) 2962–2968. doi:10.1021/ac8025702.

[53] V. Fourmond, B. Burlat, S. Dementin, P. Arnoux, M. Sabaty, S. Boiry, B. Guigliarelli, P. Bertrand, D. Pignol, C. Léger, Major Mo(V) EPR signature of *Rhodobacter sphaeroides* periplasmic nitrate reductase arising from a dead-end species that activates upon reduction. Relation to other molybdoenzymes from the DMSO reductase family, J. Phys. Chem. B 112 (48) (2008) 15478–15486. doi:10.1021/jp807092y.

[54] J. G. Jacques, V. Fourmond, P. Arnoux, M. Sabaty, E. Etienne, S. Grosse, F. Biaso, P. Bertrand, D. Pignol, C. Léger, B. Guigliarelli, B. Burlat, Reductive activation in periplasmic nitrate reductase involves chemical modifications of the Mo-cofactor beyond the first coordination sphere of the metal ion, Biochim. Biophys. Acta 1837 (2) (2014) 277–286. doi:10.1016/j.bbabio.2013.10.013.

[55] V. Fourmond, M. Sabaty, P. Arnoux, P. Bertrand, D. Pignol, C. Léger, Reassessing the strategies for trapping catalytic intermediates during nitrate reductase turnover, J. Phys. Chem. B 114 (9) (2010) 3341–3347. doi:10.1021/jp911443y.

[56] J. G. Jacques, B. Burlat, P. Arnoux, M. Sabaty, B. Guigliarelli, C. Léger, D. Pignol, V. Fourmond, Kinetics of substrate inhibition of periplasmic nitrate reductase, Biochim. Biophys. Acta 1837 (10) (2014) 1801–1809. doi:10.1016/j.bbabio.2014.05.357.

[57] R. Thomé, A. Gust, R. Toci, R. Mendel, F. Bittner, A. Magalon, A. Walburger, A sulfurtransferase is essential for activity of formate dehydrogenases in escherichia coli., J. Biol. Chem. 287 (7) (2012) 4671–4678. doi:10.1074/jbc.M111.327122.

[58] T. Reda, C. M. Plugge, N. J. Abram, J. Hirst, Reversible interconversion of carbon dioxide and formate by an electroactive enzyme, Proc. Natl Acad. Sci. USA 105 (31) (2008) 10654–10658. doi:10.1073/pnas.0801290105.

[59] J. S. McDowall, M. C. Hjersing, T. Palmer, F. Sargent, Dissection and engineering of the *Escherichia coli* formate hydrogenlyase complex., FEBS Lett. 589 (20 Pt B) (2015) 3141–3147. doi:10.1016/j.febslet.2015.08.043.

[60] V. Fourmond, C. Baffert, K. Sybirna, T. Lautier, A. Abou Hamdan, S. Dementin, P. Soucaille, I. Meynial-Salles, H. Bottin, C. Léger, Steady-state catalytic wave-shapes for 2-electron reversible electrocatalysts and enzymes, J. Am. Chem. Soc. 135 (10) (2013) 3926–3938. doi:10.1021/ja311607s.

[61] C. Feng, R. V. Kedia, J. T. Hazzard, J. K. Hurley, G. Tollin, J. H. Enemark, Effect of solution viscosity on intramolecular electron transfer in sulfite oxidase, Biochemistry 41 (18) (2002) 5816–5821. doi:10.1021/bi016059f.

[62] E. E. Ferapontova, T. Ruzgas, L. Gorton, Direct electron transfer of heme- and molybdopterin cofactor-containing chicken liver sulfite oxidase on alkanethiol-modified gold electrodes, Anal. Chem. 75 (18) (2003) 4841–4850. doi:10.1021/ac0341923.

[63] M. Sezer, R. Spricigo, T. Utesch, D. Millo, S. Leimkuehler, M. A. Mroginski, U. Wollenberger, P. Hildebrandt, I. M. Weidinger, Redox properties and catalytic activity of surface-bound human sulfite oxidase studied by a combined surface enhanced resonance raman spectroscopic and electrochemical approach, Phys. Chem. Chem. Phys. 12 (28) (2010) 7894–7903. doi:10.1039/B927226G.

[64] S. Frasca, O. Rojas, J. Salewski, B. Neumann, K. Stiba, I. M. Weidinger, B. Tiersch, S. Leimkühler, J. Koetz, U. Wollenberger, Human sulfite oxidase electrochemistry on gold nanoparticles modified electrode., Bioelectrochemistry 87 (2012) 33–41. doi:10.1016/j.bioelechem.2011.11.012.

[65] T. Zeng, S. Frasca, J. Rumschöttel, J. Koetz, S. Leimkühler, U. Wollenberger, Role of conductive nanoparticles in the direct unmediated bioelectrocatalysis of immobilized sulfite oxidase, Electroanalysis 28 (2016) 2303–2310. doi:10.1002/elan.201600246.

[66] T. Zeng, D. Pankratov, M. Falk, S. Leimkühler, S. Shleev, U. Wollenberger, Miniature direct electron transfer based sulphite/oxygen enzymatic fuel cells., Biosens Bioelectron 66 (2015) 39–42. doi:10.1016/j.bios.2014.10.080.

[67] T. Zeng, S. Leimkühler, J. Koetz, U. Wollenberger, Effective electrochemistry of human sulfite oxidase immobilized on quantum-dots-modified indium tin oxide electrode, ACS Appl. Mater. Interfaces 7 (38) (2015) 21487–21494. doi:10.1021/acsami.5b06665.

[68] P. Saengdee, C. Promptmas, T. Zeng, S. Leimkühler, U. Wollenberger, Third-generation sulfite biosensor based on sulfite oxidase immobilized on aminopropyltriethoxysilane modified indium tin oxide, Electroanalysis 29 (2017) 110–115. doi:10.1002/elan.201600566.

[69] T. D. Rapson, U. Kappler, P. V. Bernhardt, Direct catalytic electrochemistry of sulfite dehydrogenase: Mechanistic insights and contrasts with related Mo enzymes, Biochim. Biophys. Acta 1777 (10) (2008) 1319–1325. doi:10.1016/j.bbabio.2008.06.005.

[70] T. D. Rapson, U. Kappler, G. R. Hanson, P. V. Bernhardt, Short circuiting a sulfite oxidising enzyme with direct electrochemistry: active site substi-

tutions and their effect on catalysis and electron transfer., Biochim. Biophys. Acta 1807 (1) (2011) 108–118. doi:10.1016/j.bbabio.2010.09.005.

[71] G. G. Barbier, R. C. Joshi, E. R. Campbell, W. H. Campbell, Purification and biochemical characterization of simplified eukaryotic nitrate reductase expressed in *Pichia pastoris*., Protein Expr. Purif. 37 (1) (2004) 61–71. doi:10.1016/j.pep.2004.05.021.

[72] P. Kalimuthu, P. Ringel, T. Kruse, P. V. Bernhardt, Direct electrochemistry of nitrate reductase from the fungus *Neurospora crassa*., Biochim. Biophys. Acta 1857 (9) (2016) 1506–1513. doi:10.1016/j.bbabio.2016.04.001.

[73] P. Kalimuthu, K. Fischer-Schrader, G. Schwarz, P. V. Bernhardt, Mediated electrochemistry of nitrate reductase from *Arabidopsis thaliana*, J. Phys. Chem. B 117 (25) (2013) 7569–7577. doi:10.1021/jp404076w.

[74] K.-F. Aguey-Zinsou, P. V. Bernhardt, A. G. McEwan, J. P. Ridge, The first non-turnover voltammetric response from a molybdenum enzyme: direct electrochemistry of dimethylsulfoxide reductase from *Rhodobacter capsulatus*, J. Biol. Inorg. Chem. 7 (7) (2002) 879–883. doi:10.1007/s00775-002-0374-y.

[75] J. Ridge, K.-F. Aguey-Zinsou, P. Bernhardt, I. Brereton, G. Hanson, A. McEwan, Site-directed mutagenesis of dimethyl sulfoxide reductase from *Rhodobacter capsulatus*: Characterization of a Y114F mutant, Biochemistry 41 (52) (2002) 15762–15769. doi:10.1021/bi0266582.

[76] S. J. Elliott, C. Léger, H. R. Pershad, J. Hirst, K. Heffron, N. Ginet, F. Blasco, R. A. Rothery, J. H. Weiner, F. A. Armstrong, Detection and interpretation of redox potential optima in the catalytic activity of enzymes., Biochim. Biophys. Acta 1555 (1-3) (2002) 54–9. doi:10.1016/S0005-2728(02)00254-2.

[77] C. Léger, S. J. Elliott, K. R. Hoke, L. J. C. Jeuken, A. K. Jones, F. A. Armstrong, Enzyme electrokinetics: using protein film voltammetry to investigate redox enzymes and their mechanisms., Biochemistry 42 (29) (2003) 8653–62. doi:10.1021/bi034789c.

[78] K. F. Aguey-Zinsou, P. V. Bernhardt, S. Leimkühler, Protein film voltammetry of *Rhodobacter capsulatus* xanthine dehydrogenase., J. Am. Chem. Soc. 125 (50) (2003) 15352–8. doi:10.1021/ja037940e.

[79] P. V. Bernhardt, M. J. Honeychurch, A. G. McEwan, Direct electrochemically driven catalysis of bovine milk xanthine oxidase, Electrochemistry Communications 8 (2006) 257–261. doi:10.1016/j.elecom.2005.08.009.

[80] P. Kalimuthu, S. Leimkühler, P. V. Bernhardt, Xanthine dehydrogenase electrocatalysis: Autocatalysis and novel activity, J. Phys. Chem. B 115 (11) (2011) 2655–2662. doi:10.1021/jp111809f.

[81] Y. Wu, S. Hu, Direct electron transfer of xanthine oxidase and its catalytic reduction to nitrate, Anal. Chim. Acta 602 (2) (2007) 181–186. doi:10.1016/j.aca.2007.09.005.

[82] D. Shan, Y.-N. Wang, H.-G. Xue, S. Cosnier, S.-N. Ding, Xanthine oxidase/laponite nanoparticles immobilized on glassy carbon electrode: direct electron transfer and multielectrocatalysis., Biosens Bioelectron 24 (12) (2009) 3556–3561. doi:10.1016/j.bios.2009.05.009.

[83] P. V. Bernhardt, J. M. Santini, Protein film voltammetry of arsenite oxidase from the chemolithoautotrophic arsenite-oxidizing bacterium NT-26, Biochemistry 45 (9) (2006) 2804–2809. doi:10.1021/bi0522448.

[84] K. B. Male, S. Hrapovic, J. M. Santini, J. H. T. Luong, Biosensor for arsenite using arsenite oxidase and multiwalled carbon nanotube modified electrodes, Anal. Chem. 79 (20) (2007) 7831–7837. doi:10.1021/ac070766i.

[85] A. Gennaris, B. Ezraty, C. Henry, R. Agrebi, A. Vergnes, E. Oheix, J. Bos, P. Leverrier, L. Espinosa, J. Szewczyk, D. Vertommen, O. Iranzo, J.-F. Collet, F. Barras, Repairing oxidized proteins in the bacterial envelope using respiratory chain electrons., Nature 528 (7582) (2015) 409–412. doi:10.1038/nature15764.

[86] H. Adamson, A. N. Simonov, M. Kierzek, R. A. Rothery, J. H. Weiner, A. M. Bond, A. Parkin, Electrochemical evidence that pyranopterin redox chemistry controls the catalysis of YedY, a mononuclear Mo enzyme., Proc. Natl. Acad. Sci. U.S.A. 112 (47) (2015) 14506–14511. doi:10.1073/pnas.1516869112.

[87] C. C. Lee, N. S. Sickerman, Y. Hu, M. W. Ribbe, YedY: A mononuclear molybdenum enzyme with a redox-active ligand?, Chembiochem 17 (6) (2016) 453–455. doi:10.1002/cbic.201600004.

[88] M. M. Correia dos Santos, P. M. P. Sousa, M. L. S. Gonçalves, M. J. Romão, I. Moura, J. J. G. Moura, Direct electrochemistry of the *Desulfovibrio gigas* aldehyde oxidoreductase., Eur. J. Biochem. 271 (7) (2004) 1329–1338. doi:10.1111/j.1432-1033.2004.04041.x.

[89] P. Pinyou, A. Ruff, S. Pöller, S. Alsaoub, S. Leimkühler, U. Wollenberger, W. Schuhmann, Wiring of the aldehyde oxidoreductase paoabc to electrode surfaces via entrapment in low potential phenothiazine-modified redox polymers., Bioelectrochemistry 109 (2016) 24–30. doi:10.1016/j.bioelechem.2015.12.005.

[90] V. Fourmond, C. Léger, Modelling the voltammetry of adsorbed enzymes and molecular catalysts, Curr. Opin. Electrochem. 1 (2017) 110–120. doi:10.1016/j.coelec.2016.11.002.

[91] C. Léger, A. K. Jones, S. P. J. Albracht, F. A. Armstrong, Effect of a dispersion of interfacial electron transfer rates on steady state catalytic electron transport in [NiFe]-hydrogenase and other enzymes, J. Phys. Chem. B 106 (50) (2002) 13058–13063. doi:10.1021/jp0265687.

[92] V. Fourmond, C. Greco, K. Sybirna, C. Baffert, P.-H. Wang, P. Ezanno, M. Montefiori, M. Bruschi, I. Meynial-Salles, P. Soucaille, J. Blumberger, H. Bottin, L. de Gioia, C. Léger, The oxidative inactivation of FeFe hydrogenase reveals the flexibility of the H-cluster., Nat. Chem. 6 (4) (2014) 336–342. doi:10.1038/nchem.1892.

[93] A. Kubas, C. Orain, D. De Sancho, L. Saujet, M. Sensi, C. Gauquelin, I. Meynial-Salles, P. Soucaille, H. Bottin, C. Baffert, V. Fourmond, R. B. Best, J. Blumberger, C. Léger, Mechanism of O_2 diffusion and reduction in FeFe hydrogenases., Nat Chem 9 (1) (2017) 88–95. doi:10.1038/nchem.2592.

[94] G. George, J. Hilton, C. Temple, R. Prince, K. Rajagopalan, Structure of the molybdenum site of dimethyl sulfoxide reductase, J. Am. Chem. Soc. 121 (6) (1999) 1256–1266. doi:10.1021/ja982843k.

[95] R. Bray, B. Adams, A. Smith, B. Bennett, S. Bailey, Reversible dissociation of thiolate ligands from molybdenum in an enzyme of the dimethyl sulfoxide reductase family, Biochemistry 39 (37) (2000) 11258–11269. doi:10.1021/bi0000521.

[96] A. F. Bell, X. He, J. P. Ridge, G. R. Hanson, A. G. McEwan, P. J. Tonge, Active site heterogeneity in dimethyl sulfoxide reductase from *Rhodobacter capsulatus* revealed by Raman spectroscopy., Biochemistry 40 (2) (2001) 440–448. doi:10.1021/bi002065k.